

Three-dimensional Heisenberg spin glass under a weak random anisotropyV. Martin-Mayor^{1,2} and S. Perez-Gaviro^{2,3}¹*Departamento de Física Teórica I, Facultad de Ciencias Físicas, Universidad Complutense, ES-28040 Madrid, Spain*²*Instituto de Biocomputación y Física de Sistemas Complejos (BIFI), Corona de Aragón 42, Zaragoza ES-50009, Spain*³*Dipartimento di Fisica, INFN and INFN, Università di Roma La Sapienza, Ple. A. Moro 2, IT-00185 Roma, Italy*

(Received 31 May 2011; published 14 July 2011)

We perform a finite-size scaling study of the three-dimensional Heisenberg spin glass in the presence of weak random anisotropic interactions, up to lattice sizes $L = 32$. Anisotropies have a major impact on the phase transition. The chiral-glass susceptibility does not diverge due to a large anomalous dimension. It follows that the anisotropic spin glass belongs to a Universality Class different from the isotropic model, which questions the applicability of the chirality scenario.

DOI: [10.1103/PhysRevB.84.024419](https://doi.org/10.1103/PhysRevB.84.024419)

PACS number(s): 75.10.Nr, 05.50.+q, 64.60.F-, 75.40.Mg

I. INTRODUCTION

Spin glasses (SG's) are disordered magnetic alloys, widely regarded as paradigmatic complex systems.¹ The degree of anisotropy in the magnetic interactions determines whether a particular alloy is classified as a Heisenberg or an Ising SG (Ising corresponds to a limit of strong anisotropy). Experimentally, anisotropies affect significantly the glassy response to external magnetic fields and the behavior under cooling protocols.²

Theorists have privileged the study of the Ising limit, in spite of the fact that canonical SG's, e.g., CuMn or AgMn, should be rather regarded as Heisenberg with weak anisotropic interactions. Indeed, complications arise in the Heisenberg case. In addition to the standard SG ordering Heisenberg systems show as well a chiral-glass (CG) phase where *chiralities* order³ (chiralities, also named vorticities, reflect the handedness of the noncollinear spin-ordering pattern, see definitions below).

Probably motivated by failures in early numerical attempts⁴ to find a standard SG phase for Heisenberg systems, Kawamura proposed a chirality scenario expected to hold for most experimental systems.⁵ In the ideal, fully isotropic case, the standard SG critical temperature T_{SG} would be strictly zero, while chiralities would order at $T_{CG} > 0$ (spin-chirality decoupling). Yet, anisotropic interactions (dipolar, pseudodipolar, or Dzyaloshinskii-Moriya^{6,7}), albeit small, are unavoidable in experimental samples. Hence, the scenario includes a decoupling-recoupling hypothesis: weak random anisotropic interactions would recouple spins and chiralities so that $T_{CG} = T_{SG} > 0$. Indeed, the numerical work available at the time indicated that very small amounts of anisotropy lead to $T_{SG} > 0$.⁸

CG ordering may be experimentally investigated through the anomalous Hall effect. Due to spin-orbit interaction and the spin polarization of the conduction electrons, the anomalous Hall resistivity picks contributions proportional to the CG order parameter and its corresponding nonlinear susceptibility.^{9,10} The effectiveness of this tool to study noncoplanar orderings has been demonstrated in manganites¹¹ and in a geometrically frustrated pyrochlore ferromagnet.¹²

The effect of anisotropies on the critical behavior was considered by Bray and Moore,⁷ before the question of chiral ordering was raised. They predicted that these systems belong to the Ising SG Universality Class irrespective of the kind

of anisotropic interactions. However, in their analysis the assumption was made that $T_{SG} = 0$ in the isotropic limit (this assumption seemed plausible at the time, although we now know that it is incorrect).

Recent theoretical work has shown that the chirality scenario needs some revision. New simulation algorithms (allowing to thermalize at lower temperatures than pioneering work⁴), combined with modern finite-size-scaling (FSS) methods,^{13–15} have provided conclusive evidence for a standard SG ordering with $T_{SG} > 0$ for purely isotropic interactions.^{16–22} Only some controversy remains on whether T_{SG} is slightly smaller than T_{CG} ¹⁹ or rather the two are compatible within errors.²⁰ Interestingly enough, a modern-styled study seems to be still lacking for the more realistic case of a Heisenberg SG with small random anisotropy.

Here, we show that small anisotropic interactions cause that, at variance with the ideal case, the CG susceptibility no longer diverges at T_{CG} (i.e., the anomalous dimension becomes $\eta_{CG} > 2$). In the Renormalization-Group framework,¹⁵ anisotropy is a relevant perturbation. Even if in an experimental sample anisotropies are fairly small, the isotropic model is appropriate only for moderate correlation length. Closer to the critical temperature a new fixed point rules (presumably in the Ising SG Universality Class due to spin-reversal symmetry). A slow crossover¹⁵ from the Heisenberg to the anisotropic fixed point arises upon approaching the phase transition. We conjecture that this crossover explains²³ experimental claims of a nontrivial dependency of critical exponents on the anisotropy strength.^{2,24} Our results follow from a FSS analysis of equilibrium Monte Carlo simulations on lattice sizes up to $L = 32$. Data suggest that anisotropies cause a temperature range in which chiralities order while spins do not (i.e., $T_{SG} < T_{CG}$). However, due to the slow crossover, further research will be needed to dismiss spin-chirality recoupling.

The remaining part of this work is organized as follows. We define the model and describe our numerical methods in Sec. II. We address thermal equilibration, a major issue in any spin-glass simulation, in Sec. III. Our physical results are reported in Sec. IV. Finally, we give our results in Sec. V.

II. MODEL AND SIMULATIONS

Since the main types of anisotropic interactions lead to the same effective replica Hamiltonian,⁷ it is numerically

convenient to study short-range (pseudo-dipolar) interactions. We take the Edwards-Anderson model on a cubic lattice of size L with periodic boundary conditions. Heisenberg spins occupy the lattice nodes \mathbf{x} [$\vec{S}_{\mathbf{x}} = (S_{\mathbf{x}}^1, S_{\mathbf{x}}^2, S_{\mathbf{x}}^3)$, $\vec{S}_{\mathbf{x}} \cdot \vec{S}_{\mathbf{x}} = 1$]. The Hamiltonian is⁸

$$H = - \sum_{\langle \mathbf{x}, \mathbf{y} \rangle} (J_{\mathbf{x}\mathbf{y}} \vec{S}_{\mathbf{x}} \cdot \vec{S}_{\mathbf{y}} + \vec{S}_{\mathbf{x}} \cdot D_{\mathbf{x}\mathbf{y}} \vec{S}_{\mathbf{y}}) \quad (1)$$

($\langle \mathbf{x}, \mathbf{y} \rangle$: lattice nearest neighbors). The random exchange couplings $J_{\mathbf{x}\mathbf{y}}$ are Gaussian-distributed with $\overline{J_{\mathbf{x}\mathbf{y}}} = 0$ and $\overline{J_{\mathbf{x}\mathbf{y}}^2} = 1$. The random $D_{\mathbf{x}\mathbf{y}}$ are 3×3 symmetric matrices (i.e., $\vec{S}_{\mathbf{x}} \cdot D_{\mathbf{x}\mathbf{y}} \vec{S}_{\mathbf{y}} = D_{\mathbf{x}\mathbf{y}} \vec{S}_{\mathbf{x}} \cdot \vec{S}_{\mathbf{y}}$). Their matrix elements are independent and uniformly distributed in $(-D, D)$. In most of the work reported here, $D = 0.05$ (which corresponds to the best studied case⁸), but we will be presenting results for $D = 0.1$ as well.

The ideal limit of a fully isotropic Heisenberg model is recovered from Eq. (1) by setting $D = 0$. Once $D > 0$, the original O(3) symmetry, corresponding to a global spin rotation (or reflection), is lost. The only remaining symmetry for $D > 0$ is global spin inversion.

An instance of the couplings $\{J_{\mathbf{x}\mathbf{y}}, D_{\mathbf{x}\mathbf{y}}^{\mu\nu}\}$ is named a sample. For any physical quantity we first obtain the thermal average, denoted as $\langle \dots \rangle$. Only afterwards we perform the sample average (denoted by an overline).

Defining the SG and CG susceptibilities requires real replicas. We consider pairs of spin configurations, $\vec{S}_{\mathbf{x}}^a$ and $\vec{S}_{\mathbf{x}}^b$, that evolve with independent thermal noise under the same couplings and at the same temperature. The spin-overlap field is $q_{\mathbf{x}} = \vec{S}_{\mathbf{x}}^a \cdot \vec{S}_{\mathbf{x}}^b$, while its Fourier transform at wave vector \mathbf{k} is $\hat{q}_{\text{SG}}^{\mu}(\mathbf{k}) = \sum_{\mathbf{x}} q_{\mathbf{x}} e^{i\mathbf{k} \cdot \mathbf{x}} / N$. On the other hand, the local chirality is defined as:

$$\zeta_{\mathbf{x}\mu} = \vec{S}_{\mathbf{x}+\mathbf{e}_{\mu}} \cdot (\vec{S}_{\mathbf{x}} \times \vec{S}_{\mathbf{x}-\mathbf{e}_{\mu}}), \quad \mu = 1, 2, 3, \quad (2)$$

where \mathbf{e}_{μ} is the unit lattice vector along the μ axis. From Eq. (2), the chiral overlap-field is $\kappa_{\mathbf{x},\mu} = \zeta_{\mathbf{x},\mu}^a \zeta_{\mathbf{x},\mu}^b$, where the superindices a and b correspond to the replicas. Its Fourier transform is $\hat{q}_{\text{CG}}^{\mu}(\mathbf{k}) = \sum_{\mathbf{x}} \kappa_{\mathbf{x},\mu} e^{i\mathbf{k} \cdot \mathbf{x}} / N$.

The wave-vector-dependent susceptibilities are

$$\chi_{\text{SG}}(\mathbf{k}) = N \overline{\langle |\hat{q}_{\text{SG}}(\mathbf{k})|^2 \rangle}, \quad \chi_{\text{CG}}^{\mu}(\mathbf{k}) = N \overline{\langle |\hat{q}_{\text{CG}}^{\mu}(\mathbf{k})|^2 \rangle}. \quad (3)$$

The correlation length, either SG or CG, is^{15,25}

$$\xi = \frac{1}{2 \sin(k_{\min}/2)} \left[\frac{\chi(\mathbf{0})}{\chi(\mathbf{k}_{\min})} - 1 \right]^{1/2}, \quad (4)$$

where $\mathbf{k}_{\min} = (2\pi/L, 0, 0)$ or permutations.²⁶

Our simulation algorithm combines heat-bath with microcanonical overrelaxation.²⁷ Both moves generalize straightforwardly to the anisotropic case.²⁸ The mixed algorithm is effective for the isotropic Heisenberg SG^{17-20,29} and for other frustrated models.³⁰ Besides, we extrapolate to nearby temperatures using a bias-corrected³¹ data reweighting method.³² Most of our simulations were carried out with $D = 0.05$, see Table I. Nevertheless, we did as well some work for $D = 0.1$, see Table II.

TABLE I. Details of simulations with $D = 0.05$. For each lattice size and temperature we give the number of simulated samples. The last row indicates the number of Elementary Monte Carlo Steps (EMCS). The L -dependent EMCS consisted of one heat-bath full lattice sweep, followed by $5L/4$ sequential (microcanonical) overrelaxation sweeps. We took 6×10^4 measurements per sample, but for $L = 32$ (15×10^4 measurements).

$T \setminus L$	6	8	12	16	24	32
0.187	1000	1080	1000	1020	1000	1000
0.194	1000	1080	1000	1020	1000	...
0.200	1000	1080	1060	1020	1000	...
0.210	1000	1080	1000	1020	1200	1000
0.220	1000	1080	1000	1020	1080	...
0.230	1000	1080	1000	1020	1080	1000
0.240	1000	1080	1000	1020	1080	...
0.250	1000	1040	1000	1020	1000	...
EMCS $\times 10^5$	3	3	1.8	3.6	4.8	15

III. EQUILIBRATION

We considered three thermalization tests. First, we considered the identity (valid for Gaussian-distributed $J_{\mathbf{x}\mathbf{y}}$):

$$\Delta \equiv \frac{q_s - q_l}{T} + \frac{2}{z} U = 0, \quad (5)$$

where $U = - \sum_{\langle \mathbf{x}, \mathbf{y} \rangle} J_{\mathbf{x}\mathbf{y}} \langle \vec{S}_{\mathbf{x}} \cdot \vec{S}_{\mathbf{y}} \rangle / L^D$, the link-overlap is $q_l = 2 \sum_{\langle \mathbf{x}, \mathbf{y} \rangle} \langle \vec{S}_{\mathbf{x}}^a \cdot \vec{S}_{\mathbf{y}}^a \rangle \langle \vec{S}_{\mathbf{x}}^b \cdot \vec{S}_{\mathbf{y}}^b \rangle / (zL^D)$, while $q_s = 2 \sum_{\langle \mathbf{x}, \mathbf{y} \rangle} \langle (\vec{S}_{\mathbf{x}} \cdot \vec{S}_{\mathbf{y}})^2 \rangle / (zL^D)$ ($z = 6$ is the lattice coordination number). Now, both U and q_s equilibrate easily. Yet, since q_l involves two replicas, it slowly grows from zero until its equilibrium value. Thus a thermalization bias shows up as $\Delta > 0$.^{17,20,33} The time evolution of Δ , for $L = 32$ at the lowest T , is shown in Fig. 1. Second, we carried out the standard logarithmic data binning: we compare averages over the second half of the Monte Carlo history, with the second fourth, the second eighth, and so forth, finding stability for three bins. Third, we checked for compatibility among reweighting extrapolations for contiguous temperatures (our simulations at different T are statistically independent, see Fig. 2).

IV. RESULTS

Our FSS analysis compares the correlation length in units of the lattice size for pairs of lattices $(L, 2L)$.¹³⁻¹⁵ Dimensionless quantities, such as ξ/L , are functions of $L^{1/\nu}(T - T_c)$, ν being the thermal critical exponent. Thus the two curves intersect at

TABLE II. As in Table I, for our simulations with $D = 0.1$.

$T \setminus L$	6	8	12	16
0.230	300	100	100	320
0.240	300	100	100	260
0.250	300	100	100	360
0.260	200	500	500	820
0.270	200	400	500	560
0.280	120	600	500	500
EMCS $\times 10^5$	3	3	1.8	3.6

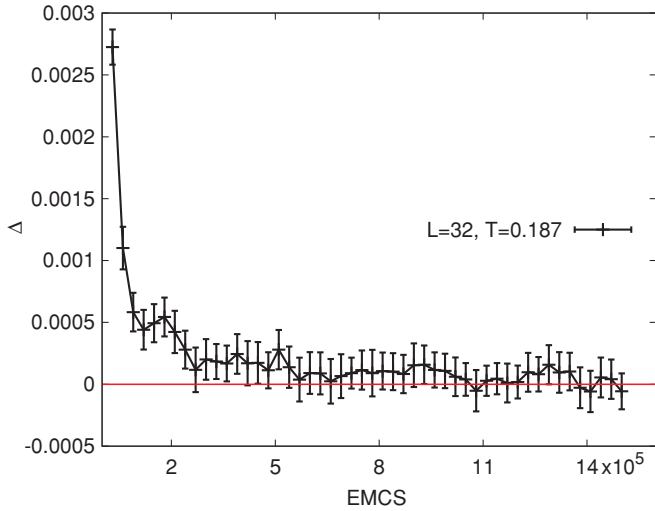


FIG. 1. (Color online) Sample-averaged Δ defined in the left-hand side of Eq. (5) vs Monte Carlo time, as computed for $L = 32$ at $T = 0.187$ and $D = 0.05$. The EMCS was defined in the caption of Table I. Each point is an average over 3000 consecutive measurements.

$T_c(L, 2L)$, see Fig. 2. $T_c(L, 2L)$ differs from T_c due to scaling corrections (but tends to it for large L , see Ref. 15). Our dimensionless quantities, ξ_{SG}/L and ξ_{CG}/L , produce two L -dependent critical temperatures $T_{SG}(L, 2L)$ and $T_{CG}(L, 2L)$. We compute the anomalous dimensions η from the scaling of the susceptibilities χ [take $\mathbf{k} = \mathbf{0}$ in Eq. (3)]. For large L and $\eta < 2$, χ diverges as $\chi \propto |T - T_c|^{-\nu(2-\eta)}$. For finite L , we consider the susceptibility ratio for χ_{CG} and χ_{SG} (the dots stand for scaling corrections):

$$\left. \frac{\chi(2L)}{\chi(L)} \right|_{T_c(L, 2L)} = 2^{2-\eta} + \dots \quad (6)$$

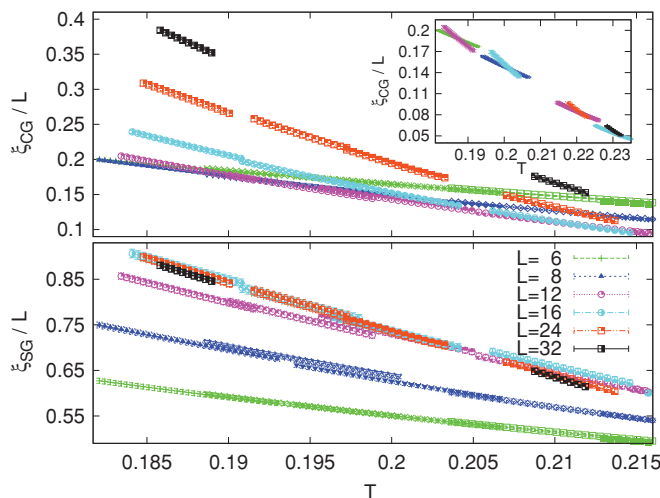


FIG. 2. (Color online) Correlation length in units of the lattice size vs T for all our system sizes at $D = 0.05$. Results for both the CG (top), and the SG sectors (bottom). Data patches correspond each to an independent simulation (we used data reweighting³²). Inset: CG intersections for pairs of sizes $(L, 2L)$. The range of T and ξ_{CG}/L differ from the main plot.

TABLE III. Size-dependent critical temperatures $T_{SG}(L, 2L)$ and $T_{CG}(L, 2L)$ and anomalous dimensions $2 - \eta_{SG}$ and $2 - \eta_{CG}$, Eq. (6), for the simulations with $D = 0.05$. Errors were obtained with jackknife.

L	$T_{SG}(L, 2L)$	$T_{CG}(L, 2L)$	$2 - \eta_{SG}$	$2 - \eta_{CG}$
6	0.251(2)	0.187(1)	2.031(11)	0.360(8)
8	0.235(1)	0.202(1)	2.131(9)	0.223(8)
12	0.207(5)	0.221(1)	2.413(46)	0.081(5)
16	0.179(10)	0.233(1)	2.639(55)	0.030(5)

We discuss first the CG sector. The inset of Fig. 2 shows an unusual feature: ξ_{CG}/L at the crossing point $T_{CG}(L, 2L)$ approaches zero for large L . This is to be expected only if $\eta \geq 2$:¹⁵ if the susceptibility does not diverge at T_c , the correlation length in Eq. (4) scales as $\xi/L \sim L^{-(\eta-2)/2}$. Nevertheless, we still find crossings when comparing lattices sizes L and $2L$, see Fig. 2 and also Ref. 34. Crossings are due to the fact that, in the large- L limit, the correlation length in Eq. (4) is divergent in the low-temperature phase. For $T < T_c$, ξ/L grows as $L^{\theta/2}$ (i.e., the correlation function at large distances r goes to a constant with corrections of order $1/r^\theta$, see, e.g., Ref. 35). Yet, the susceptibility ratio in Eq. (6) is constant for large L , even if $\eta > 2$. So, η_{CG} in Table III approaches 2 as L grows.

Besides, it is noteworthy that, in spite of the smallness of D , $T_{CG}(L, 2L)$ for $D = 0.05$ is about twice its value for the isotropic model, $T_{CG}(D = 0) \approx 0.13$.²⁰ In fact, extrapolating the data in Table III as $T_{CG}(L, 2L) = T_{CG} + A/L$ yields $T_{CG} \approx 0.26$.

To further investigate the lacking divergence of χ_{CG} at T_{CG} , we consider the integrals³⁶

$$I_k = \sum_{r=0}^{L/2} r^k C_{P,P}(r), \quad (7)$$

where $C_{P,P}(r)$ is the plane-to-plane correlation function.³⁷ Note that $\chi_{CG} \sim 2I_0$, which means that plane-to-plane correlation functions decay with r slower than the standard point-to-point correlations by a factor of r^{D-1} . The scaling behavior of the integrals (7) is $I_k \sim \text{constant}$ in the paramagnetic phase, $I_k \sim L^{k+2-\eta}$ at T_{CG} (if $k+2-\eta > 0$, otherwise it is $I_k \sim \text{constant}$), and $I_k \sim L^{D+k}$ in the CG phase. We show in Fig. 3 (top) our data for χ_{CG} (which is basically $2I_0$) and, in Fig. 3 (bottom), I_1 . Note that for $T < 0.22$, the two integrals are diverging with L . On the other hand, for $T = 0.22$ and 0.23 , I_1 grows with L , while χ_{CG} does not, as expected for $2 < \eta_{CG} < 3$.

The behavior of the SG sector is more conventional. A remarkable feature in Fig. 2 and Table III is the strong scaling corrections in $T_{SG}(L, 2L)$. We do not consider it safe to extrapolate T_{SG} to its large- L limit, as we are far from the asymptotic regime. The SG anomalous dimension takes a negative value as L grows (also found in the Ising SG, see, e.g. Ref. 13).

An intriguing feature is that T_{SG} seems smaller than T_{CG} . Indeed, see Fig. 2, at $T \approx 0.187$, where ξ_{SG}/L becomes L -independent, ξ_{CG}/L is growing fast with L . Yet, three caveats prevent us from considering this conclusion as definitive:

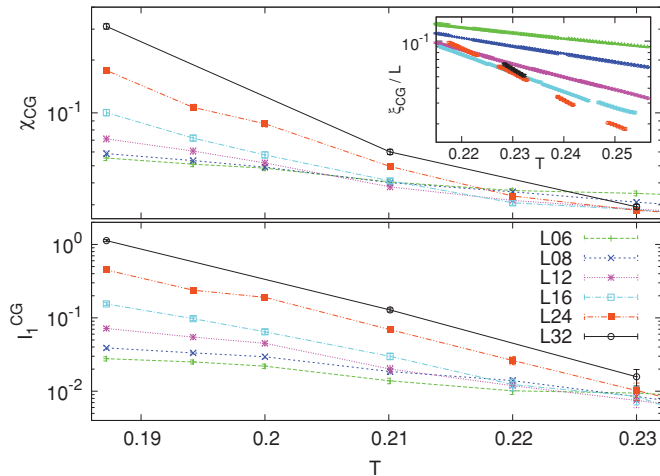


FIG. 3. (Color online) Chiral-glass susceptibility χ_{CG} (top) and I_1 integral defined in Eq. (7) (bottom) vs temperature for all our system sizes with $D = 0.05$. Lines are guides to eyes. Inset: zoom of ξ_{CG}/L vs T .

(i) our lattice sizes are still in a strong crossover regime, hence, the final picture could change as L grows, (ii) the behavior is rather marginal, meaning a larger number of samples would be needed to accurately locate T_{SG} (this is hardly surprising, given the large value of exponent ν and the small θ exponent for $d = 3$ Ising SG's), and (iii) when considering a larger anisotropy, see below, the effect seems smaller.

Indeed, we have performed further simulations with $D = 0.1$ up to $L = 16$. As shown in Fig. 4, the difference between T_{SG} and T_{CG} is less clearly defined than for $D = 0.05$. On the other hand, the chiral-glass susceptibility is not divergent at the critical point, in agreement with our results for $D = 0.05$. Consistently with that, the crossing points for ξ_{CG}/L shift to a smaller height when L grows.

V. CONCLUSIONS

In summary, we have performed a finite-size-scaling study of the 3d Heisenberg spin glass in the presence of a weak random anisotropy for lattices of size up to $L = 32$. Anisotropies cause that the CG susceptibility no longer diverges at T_{CG} , the chiralities ordering temperature. Hence, the anisotropic

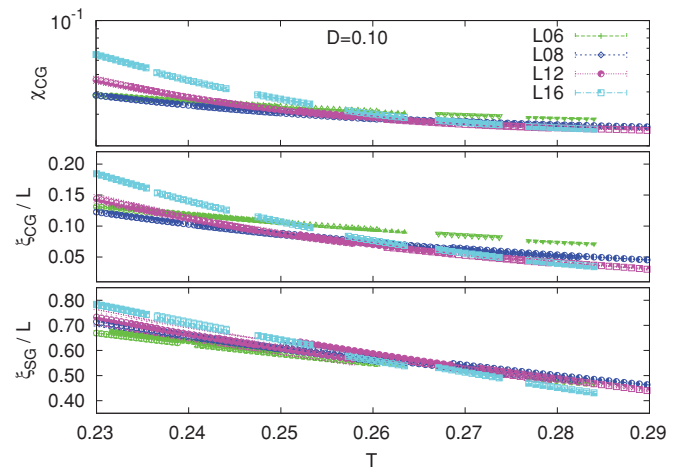


FIG. 4. (Color online) For all our lattice sizes at $D = 0.1$, we show the chiral-glass susceptibility (top), as well as the CG (center) and SG (bottom) correlation lengths in units of the system size, as a function of temperature.

system belongs to a Universality Class different from the isotropic model (probably that of Ising SG's). Besides, we found that the spin-glass ordering sets up only at $T_{SG} < T_{CG}$. The most economic scenario is that actually $T_{SG} = T_{CG}$ (the apparent difference would be due to finite-size effects). In this scenario, chiralities would merely be a composite operator (such as, say, the ninth power of the spin overlap). However, the would-be intermediate temperature region where only chiralities order should be experimentally detectable through the anomalous Hall effect. Numerical studies covering a wider range of values for the anisotropic coupling could also help to elucidate the situation.

ACKNOWLEDGMENTS

We thank A. Tarancon, G. Parisi, and P. Young for discussions. Simulations were performed at BIFI (*Terminus*, 6.6×10^5 hours of CPU time) and Red Española de Supercomputación (*Caesaraugusta*, 2.79×10^5 hours), whose staff we thank for the assistance provided. We were partly supported by MICINN (Spain) through research contract No. FIS2009-12648-C03 and (S.P.G.) through the FECYT Foundation.

¹See e.g. *Spin glasses and Random Fields*, edited by A. P. Young (World Scientific, Singapore, 1997).

²F. Bert, V. Dupuis, E. Vincent, J. Hammann, and J.-P. Bouchaud, *Phys. Rev. Lett.* **92**, 167203 (2004).

³A. Mauger, J. Villain, Y. Zhou, C. Rigaux, N. Bontemps, and J. Ferré, *Phys. Rev. B* **41**, 4587 (1990).

⁴W. L. McMillan, *Phys. Rev. B* **31**, 342 (1985); J. A. Olive, A. P. Young, and D. Sherrington, *ibid.* **34**, 6341 (1986); B. M. Morris *et al.*, *J. Phys. C* **19**, 1157 (1986).

⁵H. Kawamura, *Phys. Rev. Lett.* **68**, 3785 (1992); **80**, 5421 (1998).

⁶P. M. Levy and A. Fert, *Phys. Rev. B* **23**, 4667 (1981).

⁷A. J. Bray and M. A. Moore, *J. Phys. C* **15**, 3897 (1982).

⁸F. Matsubara, T. Iyota, and S. Inawashiro, *Phys. Rev. Lett.* **67**, 1458 (1991).

⁹G. Tataru and H. Kawamura, *J. Phys. Soc. Jpn.* **71**, 2613 (2002).

¹⁰H. Kawamura, *Phys. Rev. Lett.* **90**, 047202 (2003).

¹¹P. Matl, N. P. Ong, Y. F. Yan, Y. Q. Li, D. Studebaker, T. Baum, and G. Doubinina, *Phys. Rev. B* **57**, 10248 (1998); J. Ye, Yong Baek Kim, A. J. Millis, B. I. Shraiman, P. Majumdar, and Z. Tesanovi, *Phys. Rev. Lett.* **83**, 3737 (1999); S. H. Chun, M. B. Salamon, Y. Lyanda Geller, P. M. Goldbart, and P. D. Han, *ibid.* **84**, 757 (2000).

¹²Y. Taguchi *et al.*, *Science* **291**, 2573 (2001).

- ¹³H. G. Ballesteros, A. Cruz, L. A. Fernández, V. Martín-Mayor, J. Pech, J. J. Ruiz-Lorenzo, A. Tarancón, P. Téllez, C. L. Ullod, and C. Ungil, *Phys. Rev. B* **62**, 14237 (2000).
- ¹⁴H. G. Ballesteros *et al.*, *Phys. Lett. B* **378**, 207 (1996); **387**, 125 (1996); *Nucl. Phys. B* **483**, 707 (1997).
- ¹⁵D. Amit and V. Martin-Mayor, *Field Theory: the Renormalization Group and Critical Phenomena*, 3rd ed. (World Scientific, Singapore, 2005).
- ¹⁶L. W. Lee and A. P. Young, *Phys. Rev. Lett.* **90**, 227203 (2003).
- ¹⁷L. W. Lee and A. P. Young, *Phys. Rev. B* **76**, 024405 (2007).
- ¹⁸I. Campos, M. Cotallo-Aban, V. Martin-Mayor, S. Perez-Gaviro, and A. Tarancon, *Phys. Rev. Lett.* **97**, 217204 (2006).
- ¹⁹D. X. Viet and H. Kawamura, *Phys. Rev. Lett.* **102**, 027202 (2009).
- ²⁰L. A. Fernandez, V. Martin-Mayor, S. Perez-Gaviro, A. Tarancon, and A. P. Young, *Phys. Rev. B* **80**, 024422 (2009).
- ²¹F. Matsubara, T. Shirakura, and S. Endoh, *Phys. Rev. B* **64**, 092412 (2001); T. Nakamura and S. Endoh, *J. Phys. Soc. Jpn.* **71**, 2113 (2002).
- ²²F. Matsubara, T. Shirakura, S. Endoh, and S. Takahashi, *J. Phys. A: Math. Gen.* **36**, 10881 (2003).
- ²³The quasi long-ranged Dzyaloshinskii-Moriya interactions induce an additional crossover from mean-field to three-dimensional behavior.⁷
- ²⁴I. A. Campbell and D. Petit, *J. Phys. Soc. Jpn.* **79**, 011006 (2010).
- ²⁵F. Cooper, B. Freedman, and D. Preston, *Nucl. Phys. B* **210**, 210 (1982).
- ²⁶We will not make any distinction between the CG longitudinal or transversal correlation lengths, see, e.g., Ref. 16, since the two turn out to be compatible within errors.
- ²⁷F. R. Brown and T. J. Woch, *Phys. Rev. Lett.* **58**, 2394 (1987).
- ²⁸Equation (1) can be split as $H = \vec{h}_x \cdot \vec{S}_x + H'$, where H' is independent of \vec{S}_x , while $\vec{h}_x = \sum_{\|x-y\|=1} [J_{x,y} \vec{S}_y + D_{x,y} \vec{S}_y]$.
- ²⁹J. H. Pixley and A. P. Young, *Phys. Rev. B* **78**, 014419 (2008).
- ³⁰J. L. Alonso, A. Tarancón, H. G. Ballesteros, L. A. Fernández, V. Martín-Mayor, and A. Muñoz Sudupe, *Phys. Rev. B* **53**, 2537 (1996); E. Marinari, V. Martin-Mayor, and A. Pagnani, *ibid.* **62**, 4999 (2000).
- ³¹H. G. Ballesteros *et al.*, *Nucl. Phys. B* **512**, 681 (1998).
- ³²M. Falcioni *et al.*, *Phys. Lett. B* **108**, 331 (1982); A. M. Ferrenberg and R. H. Swendsen, *Phys. Rev. Lett.* **61**, 2635 (1988).
- ³³H. G. Katzgraber, M. Palassini, and A. P. Young, *Phys. Rev. B* **63**, 184422 (2001).
- ³⁴J. L. Alonso, A. Cruz, L. A. Fernández, S. Jiménez, V. Martín-Mayor, J. J. Ruiz-Lorenzo, and A. Tarancón, *Phys. Rev. B* **71**, 014420 (2005).
- ³⁵R. Alvarez Baños *et al.* (Janus Collaboration), *Phys. Rev. Lett.* **105**, 177202 (2010); R. Alvarez Baños *et al.* (Janus Collaboration), *J. Stat. Mech.* (2010) P06026.
- ³⁶F. Belletti *et al.* (Janus Collaboration), *Phys. Rev. Lett.* **101**, 157201 (2008).
- ³⁷For planes parallel to (say) the $\mu = 3$ lattice axis, add the correlation function for all pairs of sites $\mathbf{x} = (n_1, n_2, n_3)$ and $\mathbf{y} = (m_1, m_2, m_3)$ such that $m_3 - n_3 = r + kL$ with k integer, then divide by L^D . We average over the three lattice directions as well as over the longitudinal (weight 1/3) and the transversal (weight 2/3) correlation functions.